

# Dependence of far-field characteristics on the number of lasing modes in stadium-shaped InGaAsP microlasers

Muhan Choi<sup>1</sup>, Susumu Shinohara<sup>1</sup>, Takehiro Fukushima<sup>2</sup>, and Takahisa Harayama<sup>1</sup>

<sup>1</sup>*Department of Nonlinear Science, ATR Wave Engineering Laboratories,  
2-2-2 Hikaridai, Seika-cho, Soraku-gun, Kyoto 619-0288, Japan*

<sup>2</sup>*Department of Communication Engineering, Okayama Prefectural University, 111 Kuboki, Soja, Okayama 719-1197, Japan*

We study spectral and far-field characteristics of lasing emission from stadium-shaped semiconductor (InGaAsP) microlasers. We demonstrate that the correspondence between a lasing far-field emission pattern and the result of a ray simulation becomes better as the number of lasing modes increases. This phenomenon is reproduced in the wave calculation of the cavity modes.

PACS numbers:

Two-dimensional (2D) optical microcavities have been attracting the attention of many researchers, on one hand because of their potential applications in optical engineering [1] and on the other hand because they offer an experimental testing ground for the quantum/wave chaos theory [2]; the basic formalism for the wave description of a quantum billiard can be applied with some little modifications to the description of the light field confined in a 2D optical microcavity [3]. One of the simplest cavity shapes that are interesting from the viewpoint of the quantum/wave chaos theory is the shape called the Bunimovich stadium, as illustrated in the inset of Fig. 1 (a). This shape is well known for its mathematically proven property that a billiard ball or a ray inside the cavity exhibits fully chaotic dynamics [4].

The idea of using the stadium shape as a laser cavity has been examined both theoretically and experimentally [5, 6, 7, 8, 9, 10, 11]. Actual stadium-shaped microcavities have been fabricated using materials such as semiconductors [7, 8, 9, 10] and polymers [11]. A remarkable property that is commonly observed for relatively large cavity sizes is that the lasing emission patterns can be well explained by a ray model [7, 8, 11]. The ray model can be regarded as an open Hamiltonian system, whose openness, that is the light leakage at the cavity boundary, is described by Fresnel's law [2, 3]. A theoretical mechanism leading to the correspondence between ray and wave descriptions has been numerically investigated in Refs. [6, 7]. In the present Letter, we report experimental results on the dependence of far-field emission patterns on the number of lasing modes for stadium-shaped microlasers, revealing that the good correspondence with the result of a ray simulation is obtained when multiple modes are involved in lasing.

We carried out experiments for stadium-shaped microcavities with strained InGaAsP multiple-quantum-well separate-confinement-heterostructures, the detail of whose layer structures have been reported in Ref. [12]. The radius  $R$  of the semi-circular parts of the stadium is  $30\text{ }\mu\text{m}$ . The main difference between InGaAsP cavities and GaAs cavities used in previous works [7, 8] is that the lasing wavelength of the former,  $\lambda \approx 1558\text{ nm}$ , is almost twice as large as that of the latter,  $\lambda \approx 850$

nm. That means, for fixed  $R$ , the dimensionless size parameter  $nkR = 2n\pi R/\lambda$  for an InGaAsP cavity is almost half of that for a GaAs cavity, since the effective refractive index of InGaAsP,  $n = 3.23$ , is almost same as that of GaAs,  $n = 3.3$ . For our InGaAsP cavity,  $nkR$  becomes around 394, for which we are able to perform the wave calculation of cavity modes based on the boundary element method [13] and found that the average mode spacing is large enough to resolve individual modes with the resolution of our spectrometer.

Firstly, we report spectral characteristics of the InGaAsP laser. We electrically pump the laser at room temperature using a pulsed current of 30ns-width with

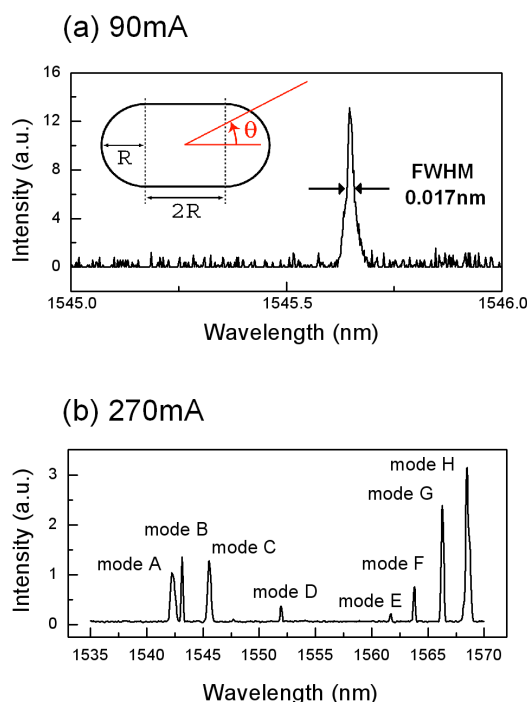


FIG. 1: Lasing spectra for the stadium-shaped InGaAsP microlaser. (a) Single-mode lasing at pumping current 90 mA. The inset shows the shape of the Bunimovich stadium. (b) Multi-mode lasing at 270 mA.

1 % duty cycle. In our experiment, setting the pulse width short is crucial for maintaining thermal stability necessary for the achievement of single-mode lasing. The lasing threshold current is measured as 81 mA. The laser shows stable single-mode lasing for the pumping current below 132 mA. We show the spectrum data for single-mode lasing at the pumping current 90 mA in Fig. 1 (a). The achievement of the single-mode lasing is assured by two experimental evidence. One is that the FWHM of the peak in Fig. 1 (a) is 0.017 nm, which is less than the theoretical estimate of the average mode spacing 0.027 nm. This estimate is based on the analysis of 54 cavity modes for a stadium-shaped cavity with  $nkR \approx 394$ . The cavity modes are solutions of the Maxwell equations for a stadium-shaped cavity without gain [13]. The other evidence is that, below 132 mA, the far-field emission pattern does not change for the increase of the pumping current, except for overall linear intensity growth. At the pumping current 132 mA, another lasing mode emerges and the number of lasing modes grows continuously as the pumping current increases. For instance, at 270 mA, we observed 8 lasing modes in the spectrum as shown in Fig. 1 (b).

Next, we report far-field characteristics. Figures 2 (a) and 2 (b) show the far-field patterns for single-mode lasing at 100 mA and for multi-mode lasing at 270 mA, respectively, where the result of a ray simulation is also plotted. We note that the intensity is normalized in both far-field patterns so that the integration of the pattern over all angles becomes unity. Moreover, spatial oscillations smaller than 0.8 degrees are smeared out because of the resolution of our measurement. One can see that the correspondence of the experimental far-field pattern with the result of a ray simulation becomes better in the multi-mode lasing case than in the single-mode lasing case. In Fig. 2 (a), clear discrepancies from the result of a ray simulation is observed such as the appearance of peaks at  $\theta = \pm 30$  degrees.

Investigating the far-field patterns of each of the 54 cavity modes, we found that the appearance of such a discrepancy is not an exceptional but a common feature of the individual cavity modes [7]. We show a typical example of the far-field pattern of a cavity mode in Fig. 2 (c). The far-field pattern of the multi-mode lasing can be approximated by the average of the far-field patterns of multiple cavity modes. The pattern obtained by averaging 8 cavity modes and that obtained by averaging 54 cavity modes are shown in Fig. 2 (d). In both cases, one can see that the correspondence with the result of a ray simulation becomes better than in the case of a single cavity mode. Moreover, it can be confirmed that, by increasing the number of the averaged modes, the averaged result converges to the result of a ray simulation.

The experimental far-field patterns shown in Fig. 2 (a) and 2 (b) are measured by a photodetector. Using a monochromator instead, we can measure the far-field patterns for individual lasing modes for the multi-mode lasing case for the pumping current 270 mA. In Fig. 3, we

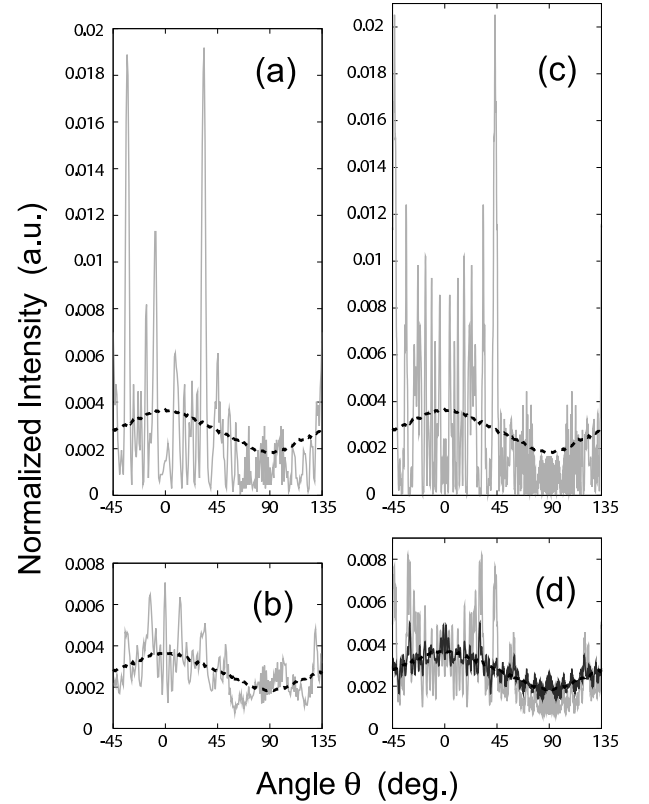


FIG. 2: Far-field patterns: experimental ((a) and (b)) vs. theoretical ((c) and (d)) with ray simulation data (broken curves). (a) Experimental data for the pumping current 100 mA. (b) Experimental data for 270 mA. These experimental data are measured by a photodetector. Spatial oscillations smaller than 0.8 degrees are smeared out because of the resolution of our measurement. (c) Wave calculation data of a single cavity mode. (d) Wave calculation data of the average of multiple cavity modes; the number of averaged modes is 8 in the gray curve and 54 in the black curve. We note that the wave calculation and the ray simulation are carried out assuming the transverse-electric polarization.

plot the far-field patterns corresponding to 6 dominant lasing modes in Fig. 1 (b), measured by a monochromator whose transmission band width is 0.01 nm. We note that rapid spatial oscillations smaller than 0.24 degrees are smeared out in the measurement. As expected from the analysis of the individual cavity modes, each of the lasing modes is found to have a less similar pattern with the result of a ray simulation. We note that mode C in Fig. 3 is nothing but the mode shown in Fig. 2 (a). The agreement of the far-field pattern of mode C and that of the single-mode lasing at 100 mA convinces us the consistency between the measurements by the photodetector and by the monochromator. The existence of a variety of patterns in lasing modes as shown in Fig. 3 is contrasted with the previous work on the quadrupole-deformed cavity [14], where the far-field pattern of each of the lasing modes is found to exhibit a good agreement with the result of a ray simulation. On the basis of our present

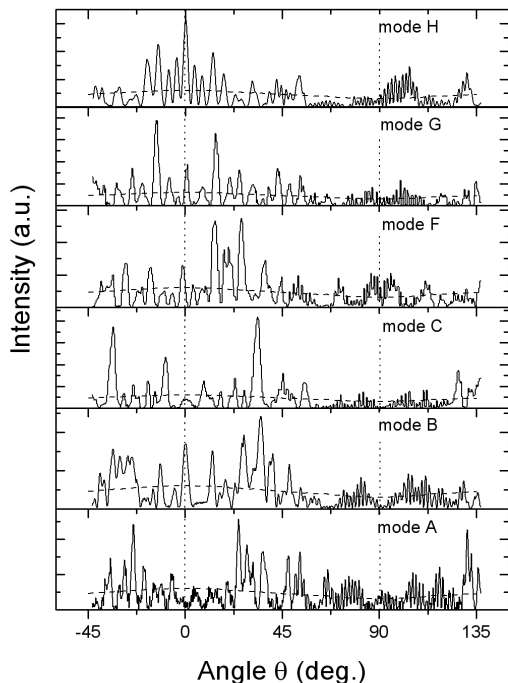


FIG. 3: Far-field patterns for the 6 dominant lasing modes for the pumping current 270 mA. The data are measured by a monochromator. The labeling of the lasing modes corresponds to that in Fig. 1 (b). The result of a ray simulation is plotted in dashed curves.

result and previous theoretical analysis [7], we conclude that in general (i.e., for a generic cavity shape with an arbitrary refractive index) the good correspondence with the result of a ray simulation can not always be obtained for a single lasing mode, but can be obtained as a result of multi-mode lasing.

Lastly, we remark on the asymmetry of the far-field patterns observed in Figs. 2 (a) and 3. In theory, the far-field patterns of individual cavity modes obey the  $C_{2v}$  symmetry of the stadium shape. However, some of the measured patterns in Figs. 2 (a) and 3 (e.g. mode F) exhibit noticeable asymmetries. It is difficult to attribute these asymmetries to extrinsic imperfections involved in the fabrication and measurement, since we have also observed a rather symmetric pattern (e.g. mode A) for the same cavity. A plausible explanation is that an asymmetric lasing mode corresponds not to a single cavity mode but multiple cavity modes with their frequencies locked to a single frequency. It has been demonstrated experimentally and numerically that multiple frequency-locked modes can generate asymmetric emission patterns [5].

In summary, performing experiments on stadium-shaped InGaAsP microlasers, we show that the correspondence of the lasing far-field pattern with the result of a ray model becomes better by increasing the number of lasing modes. The discrepancies from the result of a ray model measured in the far-field patterns of individual lasing modes are attributed as an intrinsic property of cavity modes.

The work at ATR was supported in part by the National Institute of Information and Communications Technology of Japan.

- 
- [1] K. J. Vahala, *Nature* **424**, 839 (2003).
  - [2] J. U. Nöckel and A. D. Stone, *Nature* **385**, 45 (1997).
  - [3] For example, H. G. L. Schwefel, H. E. Türeci, A. D. Stone and R. K. Chang, in *Optical Processes in Microcavities*, edited by K. Vahala, World Scientific, Singapore (2005).
  - [4] L. A. Bunimovich, *Commun. Math. Phys.* **65**, 295 (1977).
  - [5] T. Harayama, P. Davis and K. S. Ikeda, *Phys. Rev. Lett.* **90**, 063901 (2003); T. Harayama, T. Fukushima, S. Sunada and K. S. Ikeda, *Phys. Rev. Lett.* **91**, 073903 (2003); S. Shinohara, S. Sunada, T. Harayama and K. S. Ikeda, *Phys. Rev. E* **71**, 036203 (2005); S. Sunada, T. Harayama and K. S. Ikeda, *Phys. Rev. E* **71**, 046209 (2005); T. Harayama, S. Sunada and K. S. Ikeda, *Phys. Rev. A* **72**, 013803 (2005).
  - [6] S. Shinohara, T. Harayama, H. E. Türeci, and A. D. Stone, *Phys. Rev. A* **74**, 033820 (2006); S. Shinohara and T. Harayama, *Phys. Rev. E* **75**, 036216 (2007).
  - [7] S. Shinohara, T. Fukushima and T. Harayama, to appear in *Phys. Rev. A* (2008).
  - [8] T. Fukushima and T. Harayama, *IEEE J. Quantum Electron.* **10**, 1039 (2004).
  - [9] W. Fang, H. Cao, and G. S. Solomon, *Appl. Phys. Lett.* **90**, 081108 (2007).
  - [10] H. -G. Park, F. Qian, C. J. Barrelet and Y. Li, *Appl. Phys. Lett.* **91**, 251115 (2007).
  - [11] M. Lebental, J. S. Lauret, R. Hierle, and J. Zyss, *Appl. Phys. Lett.* **88**, 031108 (2006); M. Lebental, J. S. Lauret, J. Zyss, C. Schmit, and E. Bogomolny, *Phys. Rev. A* **75**, 033806 (2007).
  - [12] T. Fukushima, T. Tanaka and T. Harayama, *Appl. Phys. Lett.*, **87**, 191103 (2005).
  - [13] J. Wiersig, *J. Opt. A, Pure Appl. Opt.* **5**, 53 (2003).
  - [14] J.-B. Shim, S.-B. Lee, J. Yang, S. Moon, J.-H. Lee, K. An, H.-W. Lee, and S. W. Kim, *J. Phys. Soc. Phys. Jpn.* **76**, 114005 (2007).